Binuclear Co(II), Ni(II), Cu(II) and Zn(II) complexes with Schiff-bases derived from crown ether platforms: rare examples of ether oxygen atoms bridging metal centers

Lea Vaiana, Marta Mato-Iglesias, David Esteban-Gómez, Carlos Platas-Iglesias, Andrés de Blas[*], Teresa Rodríguez-Blas[†]

Departamento de Química Fundamental, Facultad de Ciencias, Universidade da Coruña, Campus da Zapateira s/n 15071 A Coruña, Spain

How to cite:

Abstract

Bibracchial lariat ethers L^3 and L^4, derived from the condensation of *N,N′*-bis(2-aminobenzyl)-1,10-diaza-15-crown-5 or *N,N′*-bis(2-aminobenzyl)-4,13-diaza-18-crown-6 with salicylaldehyde, form binuclear complexes with Co(II), Ni(II), Cu(II) and Zn(II). Our studies show that the different denticity and crown moiety size of the two related receptors give rise to important differences on the structures of the corresponding complexes. Single crystal X-ray diffraction analysis shows that the $[Ni_2(L^3)(H_2O)_2]^{2+}$ and $[Cu_2(L^3)(NO_3)]^+$ complexes constitute a rare example in which an oxygen atom of the crown moiety is bridging the two six coordinate metal ions. In contrast, none of the oxygen atoms of the crown moiety is acting as a bridging donor atom in the $[Co_2(L^4)(CH_3CN)_2]^{2+}$, $[Cu_2(L^4)]^{2+}$ and $[Zn_2(L^4)]^{2+}$ complexes. This is attributed to the larger size the crown moiety and the higher denticity of L^4 compared to L^3. In $[Co_2(L^4)(CH_3CN)_2]^{2+}$ the metal ions show a distorted octahedral coordination, while in the Cu(II) and Zn(II) analogues the metal ions are five-coordinated in a distorted trigonal bipyramidal environment. In $[Cu_2(L^3)(NO_3)]^+$ the coordinated nitrate anion acts as a bidentate bridging ligand, which results in the formation of a 1D coordination polymer.

Keywords: macrocyclic ligands; crystal structures; Schiff-bases; binuclear complexes; crown ethers; transition-metal complexes

---

[*] andres.blas@udc.es
[†] teresa.rodriguez.blas@udc.es

1. Introduction

Transition-metal complexes of Schiff-base ligands have been proven to be useful for the design of molecular ferromagnets, catalysts for many organic reactions, models for the active sites in metalloenzymes, optical and luminescent materials, or DNA cleavage reagents [1-5]. A rational control of the nuclearity of transition-metal complexes is important to design systems with the desired properties, as some of these applications require the presence of more than one metal center in the particular complex. Indeed, binuclear complexes may have very different reactivity than mononuclear counterparts, thereby enabling transformations inaccessible to single metal ions [6]. For instance, nucleic acid hydrolysis is postulated to be facilitated by the cooperative action of two metal ions [7]. Furthermore, bi- or oligonuclear complexes containing transition metals may be formed by bridging ligands that can mediate magnetic interactions between paramagnetic metal ions [8].

In previous works we have carried out studies to assess the different complexation capabilities of the bibracchial lariat ethers L^1 and L^2 (Scheme 1) towards divalent metal ions such as Zn(II) [9], Ba(II) [10], Pb(II) and Cd(II) [11-13]. We have also demonstrated that L^2 is able to form binuclear complexes with metal ions such as Ni(II), Co(II) and Cu(II) [14], while L^1 forms mononuclear complexes with first row transition metal ions such as Mn(II), Co(II), Ni(II) or Cu(II) [15,16]. These complexes represent unusual examples of structurally characterized seven coordinate (pentagonal bipyramidal) complexes of first row transition-metal ions. Both L^1 and L^2 can react with different monoaldehydes to form Schiff-bases with interesting coordination properties towards Pb(II) and the trivalent lanthanide ions [17-19]. Furthermore, reaction of L^1 and L^2 with dialdehydes led to the formation of macrobicyclic structures that are useful for the coordination of both cations and anions [20-22]. In this paper, we report a series of binuclear Co(II), Ni(II), Cu(II) and Zn(II) complexes with ligands L^3 and L^4, which are obtained by reaction of the corresponding precursor (L^1 or L^2) with salicylaldehyde.
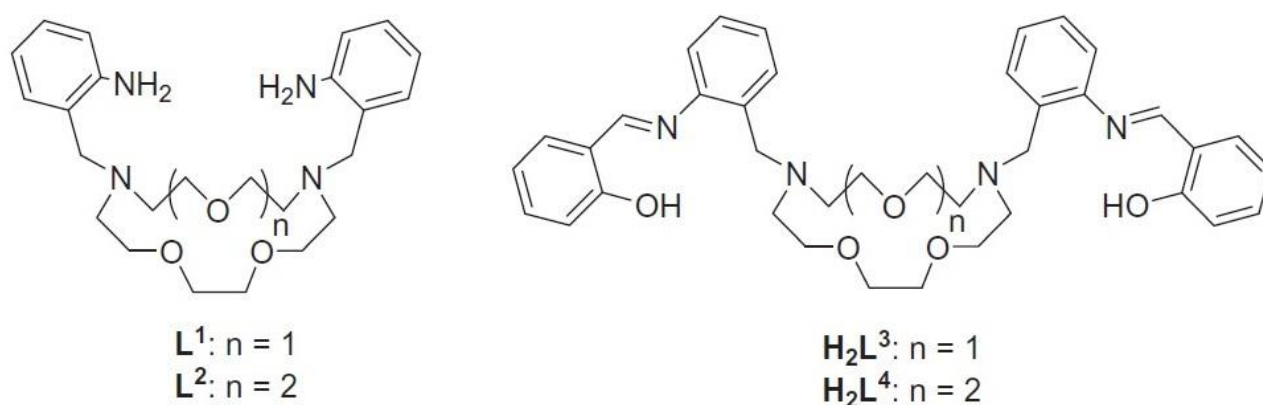
Scheme 1.

2. Experimental

2.1. Reagents

The diamine precursors N,N'-bis(2-aminobenzyl)-1,10-diaza-15-crown-5 (L^1) and N,N'-bis(2-aminobenzyl)-4,13-diaza-18-crown-6 (L^2) were prepared as previously described by us [16,23]. All other chemicals were purchased from commercial sources and used without further purification. Solvents were of reagent grade purified by the usual methods.

2.2. Synthesis

2.2.1. $[Co_2(L^3)](ClO_4)_2 \cdot C_3H_8O \cdot H_2O$ (1)

Triethylamine (65 μL, 0.466 mmol) was added with stirring to a solution of salicylaldehyde (43 μL, 0.400 mmol) in 2-propanol (10 mL). The mixture was refluxed for 1 h, and then a solution of N,N'-bis(2-aminobenzyl)-1,10-diaza-15-crown-5 (L^1) (0.086 g; 0.201 mmol) in 20 mL of 2-propanol was added. The resultant solution was refluxed for 2 h, and then a solution of $Co(ClO_4)_2 \cdot 6H_2O$ (0.149 g, 0.407 mmol) in 2-propanol (12 mL) was added. The mixture was heated to reflux with stirring for 4 h and the orange precipitate formed was collected by filtration and air-dried. Yield: 0.115 g (56%). *Anal.* Calc. for $C_{38}H_{42}Cl_2Co_2N_4O_{13} \cdot C_3H_8O \cdot H_2O$: C, 47.83; H, 5.09; N, 5.44. Found: C, 47.99; H, 5.18; N, 5.61%. FAB-MS: m/z (%BPI) = 851(53) $[Co_2(L^3)(ClO_4)]^+$, 694(100) $[Co(HL^3)]^+$. IR (KBr discs): 1611 $v(C{=}N)_{imine}$; 1086 $v_{as}(Cl{-}O)$; 624 $\delta_{as}(O{-}Cl{-}O)$ cm^{-1}.

2.2.2. $[Ni_2(L^3)](ClO_4)_2 \cdot 4H_2O$ (2)

The preparation of the green microcrystalline complex followed the same procedure described for **1** by using a solution of $Ni(ClO_4)_2 \cdot 6H_2O$ (0.148 g, 0.405 mmol) in 18 mL of 2-propanol. Yield: 0.096 g (47%). *Anal.* Calc. for $C_{38}H_{42}Cl_2N_4Ni_2O_{13} \cdot 4H_2O$: C, 44.61; H, 4.93; N, 5.48. Found: C, 44.75; H, 5.26; N, 5.32%. FAB-MS: m/z (%BPI) = 851(42) $[Ni_2(L^3)(ClO_4)]^+$, 693(72) $[Ni(HL^3)]^+$. IR (KBr discs): 1606 $v(C{=}N)_{imine}$; 1085 $v_{as}(Cl{-}O)$; 626 $\delta_{as}(O{-}Cl{-}O)$ cm^{-1}.

2.2.3. $[Cu_2(L^3)](ClO_4)_2 \cdot 2H_2O$ (3)

The preparation of the green complex followed the same procedure described for **1** by using a solution of $Cu(ClO_4)_2 \cdot 6H_2O$ (0.147 g, 0.396 mmol) in 30 mL of 2-propanol. Yield: 0.171 g (86%). *Anal.* Calc. for $C_{38}H_{42}Cl_2Cu_2N_4O_{13} \cdot 2H_2O$: C, 45.79; H, 4.65; N, 5.62. Found: C, 46.14; H, 4.66; N, 5.50%. FAB-MS: m/z (%BPI) = 861(100) $[Cu_2(L^3)(ClO_4)]^+$, 698(13) $[Cu(HL^3)]^+$. IR (KBr discs): 1608 $v(C{=}N)_{imine}$; 1088 $v_{as}(Cl{-}O)$; 626 $\delta_{as}(O{-}Cl{-}O)$ cm^{-1}.

2.2.4. $[Zn_2(L^3)](ClO_4)_2 \cdot 2H_2O$ (4)

The preparation of the complex followed the same procedure described for **1** by using a solution of $Zn(ClO_4)_2 \cdot 6H_2O$ (0.151 g, 0.405 mmol) in 5 mL of 2-propanol. Yield: 0.101 g (51%). *Anal.* Calc. for $C_{38}H_{42}Cl_2N_4O_{13}Zn_2 \cdot 2H_2O$: C, 45.62; H, 4.63; N, 5.60. Found: C, 45.81; H, 5.00; N, 5.45%. FAB-MS: m/z (%BPI) = 865(87) $[Zn_2(L^3)(ClO_4)]^+$, 699(97) $[Zn(HL^3)]^+$. IR (KBr discs): 1610 $v(C{=}N)_{imine}$; 1091 $v_{as}(Cl{-}O)$; 624 $\delta_{as}(O{-}Cl{-}O)$ cm^{-1}.

2.2.5. $[Co_2(L^3)](NO_3)_2 \cdot C_3H_8O \cdot H_2O$ (5)

The preparation followed the same procedure described for **1** by using a solution of $Co(NO_3)_2 \cdot 6H_2O$ (0.118 g, 0.406 mmol) in 8 mL of 2-propanol. The resultant solution was filtered while hot and left to evaporate at room temperature for several days. The orange microcrystalline solid formed was collected by filtration and air-dried. Yield: 0.098 g (51%). *Anal.* Calc. for $C_{38}H_{42}Co_2N_6O_{11} \cdot 4H_2O$: C, 48.11; H, 5.31; N, 8.86. Found: C, 48.00; H, 5.03; N, 8.62%. FAB-MS: m/z (%BPI) = 814(25) $[Co_2(L^3)(NO_3)]^+$, 694(100) $[Co(HL^3)]^+$. IR (KBr discs): 1606 $v(C{=}N)_{imine}$; 1384 $v(N{-}O)$ cm^{-1}.

2.2.6. $[Ni_2(L^3)](NO_3)_2 \cdot 5H_2O$ (6a)

The preparation of the yellow microcrystalline complex followed the same procedure described for **1** by using a solution of $Ni(NO_3)_2 \cdot 6H_2O$ (0.117 g, 0.402 mmol) in 7 mL of 2-propanol. Yield: 0.092 g (48%). *Anal.* Calc. for $C_{38}H_{42}N_6Ni_2O_{11} \cdot 5H_2O$: C, 47.24; H, 5.42; N, 8.70. Found: C, 47.66; H, 5.60; N, 8.54%. FAB-MS: m/z (%BPI) = 812(75) $[Ni_2(L^3)(NO_3)]^+$, 693(100) $[Ni(HL^3)]^+$. IR (KBr discs): 1606 $v(C{=}$

N)$_{imine}$; 1382 v(N–O) cm^{-1}. Slow evaporation of the mother liquor gave single crystals of formula [Ni$_2$(L^3)(H$_2$O)$_2$]$_2$(Et$_3$NH)(NO$_3$)$_5$·4H$_2$O (**6b**).

2.2.7. [Cu$_2$(L^3)](NO$_3$)$_2$·2H$_2$O (7a)

The preparation of the green complex followed the same procedure described for **1** by using a solution of Cu(NO$_3$)$_2$·6H$_2$O (0.096 g, 0.397 mmol) in 30 mL of 2-propanol. Yield: 0.118 g (64%). *Anal.* Calc. for C$_{38}$H$_{42}$Cu$_2$N$_6$O$_{11}$·2H$_2$O: C, 49.51; H, 5.03; N, 9.12. Found: C, 50.22; H, 4.94; N, 8.67%. FAB-MS: m/z (%BPI) = 822(100) [Cu$_2$(L^3)(NO$_3$)]$^+$, 698(7) [Cu(HL^3)]$^+$. IR (KBr discs): 1608 v(C=N)$_{imine}$; 1384 v(N–O) cm^{-1}. X-ray quality crystals of formula [Cu$_2$(L^3)(NO$_3$)$_2$]·2CH$_3$CN (**7b**) were grown by slow diffusion of diethyl ether into a solution of **7a** in acetonitrile.

2.2.8. [Zn$_2$(L^3)](NO$_3$)$_2$·3H$_2$O (8)

The preparation of the yellow complex followed the same procedure described for **1** by using a solution of Zn(NO$_3$)$_2$·6H$_2$O (0.117 g, 0.402 mmol) in 12 mL of 2-propanol. Yield: 0.106 g (56%). *Anal.* Calc. for C$_{38}$H$_{42}$N$_6$O$_{11}$Zn$_2$·3H$_2$O: C, 48.37; H, 5.13; N, 8.91. Found: C, 47.73; H, 4.77; N, 8.89%. FAB-MS: m/z (%BPI) = 828(38) [Zn$_2$(L^3)(NO$_3$)]$^+$, 699(30) [Zn(HL^3)]$^+$. IR (KBr discs): 1614 v(C=N)$_{imine}$; 1385 v(N–O) cm^{-1}.

2.2.9. [Co$_2$(L^4)](ClO$_4$)$_2$·H$_2$O (9a)

Triethylamine (65 μL, 0.466 mmol) was added with stirring to a solution of salicylaldehyde (43 μL, 0.400 mmol) in 2-propanol (10 mL). The mixture was refluxed for 60 min and then a solution of *N,N'*-bis(2-aminobenzyl)-4,13-diaza-18-crown-6 (**L^2**) (0.095 g; 0.201 mmol) in 22 mL of 2-propanol was added. The resultant solution was refluxed for 4 h, and then a solution of Co(ClO$_4$)$_2$·6H$_2$O (0.156 g, 0.426 mmol) in 2-propanol (4 mL) was added. The mixture was heated to reflux with stirring for 4 h. The orange precipitate formed was collected by filtration and air-dried. Yield: 0.181 g (89%). *Anal.* Calc. for C$_{40}$H$_{46}$Cl$_2$Co$_2$N$_4$O$_{14}$·H$_2$O: C, 47.40; H, 4.77; N, 5.53. Found: C, 47.58; H, 4.75; N, 5.58%. FAB-MS: m/z (%BPI) = 895(13) [Co$_2$(L^4)(ClO$_4$)]$^+$, 738(45) [Co(HL^4)]$^+$. IR (KBr discs): 1606 v(C=N)$_{imine}$; 1081 v_{as}(Cl–O); 623 δ_{as}(O–Cl–O) cm^{-1}. X-ray quality crystals of formula [Co$_2$(L^4)(CH$_3$CN)$_2$](ClO$_4$)$_2$ (**9b**) were grown by slow evaporation of a solution of **9a** in acetonitrile.

2.2.10. [Ni$_2$(L^4)](ClO$_4$)$_2$·2H$_2$O·2C$_3$H$_8$O (10)

The preparation of the green complex followed the same procedure described for **9** by using a solution of Ni(ClO$_4$)$_2$·6H$_2$O (0.146 g, 0.399 mmol) in 7 mL of 2-propanol. Yield: 0.085 g (37%). *Anal.* Calc. for C$_{40}$H$_{46}$Cl$_2$N$_4$Ni$_2$O$_{14}$·2H$_2$O·2C$_3$H$_8$O: C, 47.99; H, 5.78; N, 4.87. Found: C, 47.76; H, 5.90; N, 4.97%. FAB-MS: m/z (%BPI) = 895(100) [Ni$_2$(L^4)(ClO$_4$)]$^+$, 737(8) [Ni(HL^4)]$^+$. IR (KBr discs): 1608 v(C=N)$_{imine}$; 1083 v_{as}(Cl–O); 626 δ_{as}(O–Cl–O) cm^{-1}.

2.2.11. [Zn$_2$(L^4)](ClO$_4$)$_2$ (11)

The preparation of the yellow complex followed the same procedure described for **9** by using a solution of Zn(ClO$_4$)$_2$·6H$_2$O (0.149 g, 0.400 mmol) in 3 mL of 2-propanol. Yield: 0.135 g (67%). *Anal.* Calc. for C$_{40}$H$_{46}$Cl$_2$N$_4$O$_{14}$Zn$_2$: C, 47.64; H, 4.60; N, 5.56. Found: C, 47.32; H, 5.05; N, 5.65%. FAB-MS: m/z (%BPI) = 907(9) [Zn$_2$(L^4)(ClO$_4$)]$^+$, 743(30) [Zn(HL^4)]$^+$. IR (KBr discs): 1610 v(C=N)$_{imine}$; 1091 v_{as}(Cl–O); 624 δ_{as}(O–Cl–O) cm^{-1}. X-ray quality crystals were grown by slow diffusion of diethyl ether into a solution of **11** in acetonitrile.

2.2.12. [Co₂(L⁴)](NO₃)₂·H₂O (12)

The preparation of the orange complex followed the same procedure described for **9** by using a solution of Co(NO₃)₂·6H₂O (0.119 g, 0.409 mmol) in 10 mL of 2-propanol. Yield: 0.146 g (78%). *Anal.* Calc. for $C_{40}H_{46}Co_2N_6O_{12}·H_2O$: C, 51.18; H, 5.15; N, 8.95. Found: C, 51.35; H, 5.37; N, 9.22%. FAB-MS: m/z (%BPI) = 858(7) [Co₂(L⁴)(NO₃)]⁺, 738(53) [Co(HL⁴)]⁺. IR (KBr discs): 1610 v(C=N)$_{imine}$; 1384 v(N–O).

2.2.13. [Ni₂(L⁴)](NO₃)₂·3H₂O (13)

The preparation followed the same procedure described for **9** by using a solution of Ni(NO₃)₂·6H₂O (0.118 g, 0.405 mmol) in 7 mL of 2-propanol. Yield: 0.112 g (57%). *Anal.* Calc. for $C_{40}H_{46}N_6Ni_2O_{12}·3H_2O$: C, 49.31; H, 5.38; N, 8.63. Found: C, 49.19; H, 5.42; N, 8.47%. FAB-MS: m/z (%BPI) = 856(100) [Ni₂(L⁴)(NO₃)]⁺, 737(20) [Ni(HL⁴)]⁺. IR (KBr discs): 1608 v(C=N)$_{imine}$; 1384 v(N–O).

2.2.14. [Cu₂(L⁴)](NO₃)₂·H₂O (14a)

The deep green complex was prepared as previously described [16]. X-ray quality crystals of formula [Cu₂(L⁴)](NO₃)₂ (**14b**) were grown by slow diffusion of diethyl ether into a solution of **14a** in acetonitrile.

2.2.15. [Zn₂(L⁴)](NO₃)₂·3H₂O (15)

The preparation followed the same procedure described for **9** by using a solution of Zn(NO₃)₂·6H₂O (0.119 g, 0.400 mmol) in 5 mL of 2-propanol. Yield: 0.174 g (88%). *Anal.* Calc. for $C_{40}H_{46}N_6O_{12}Zn_2·3H_2O$: C, 48.64; H, 5.31; N, 8.51. Found: C, 48.70; H, 5.25; N, 8.85%. FAB-MS: m/z (%BPI) = 681(22) [H₂L⁴+H]⁺. IR (KBr discs): 1614 v(C=N)$_{imine}$; 1385 v(N–O).

2.3. Measurements

Elemental analyses were carried out on a Carlo Erba 1180 elemental analyser. FAB-mass spectra were recorded on a Fisons Quatro mass spectrometer with a Cs ion gun using 3-nitrobenzyl alcohol as matrix. ¹H and ¹³C NMR spectra were run on a Bruker Avance 300 using acetonitrile-d₃ as solvent. IR spectra were recorded, as KBr discs, using a Bruker Vector 22 spectrophotometer.

2.4. X-ray crystallography

Three-dimensional X-ray data were collected on Bruker SMART 1000 CCD (compounds **6b**, **9b** and **11**), Bruker-Nonius FR591-Kappa CCD 2000 (**7b**) or Bruker X8 APEXII CCD diffractometers (**14b**) by the omega and phi scan method. Reflections were measured from a hemisphere of data collected of frames each covering 0.3° in omega. The reflections measured were corrected for Lorentz and polarization effects and for absorption by semi-empirical methods based on symmetry-equivalent and repeated reflections. The solution, refinement and analysis of the single crystal X-ray diffraction data was performed with wingx suite for small molecule single-crystal crystallography [24]. The structures were solved by Patterson methods with dirdif99 [25] (**6b** and **14b**), or direct methods with shelxs-97 [27] (**9b** and **11**) or sir2002 [26] (**7b**), and refined by full-matrix least-squares methods on F^2 with shelx97 [27]. The hydrogen atoms were included in calculated positions and refined by using a riding mode. Refinement converged with allowance for thermal anisotropy of all non-hydrogen atoms. Crystal data and details on data collection and refinement are summarized in Table 1, Table 2.

Table 1. Crystal data and structure refinement for **6b** and **7b**.

	6b	7b
Empirical formula	$C_{82}H_{116}N_{14}Ni_4O_{33}$	$C_{42}H_{48}Cu_2N_8O_{11}$
Molecular weight	2060.73	967.96
Temperature (K)	100.0(2)	120.0(2)
Wavelength (Å)	0.71073	0.71073
Crystal system	triclinic	triclinic
Space group	$P1^-$	$P1^-$
a (Å)	12.248(1)	10.5319(5)
b (Å)	16.675(2)	11.8784(4)
c (Å)	23.233(2)	17.7500(7)
α (°)	95.925(2)	93.367(3)
β (°)	96.473(2)	96.008(3)
γ (°)	103.102(2)	105.385(2)
V (Å^3)	4550.9(8)	2120.55(15)
$F(0\ 0\ 0)$	2164	1004
Z	2	2
Calculated density (g cm^{-3})	1.504	1.516
Absorption coefficient (mm^{-1})	0.907	1.837
θ Range for data collection (°)	1.45–28.28	2.51–72.72
R_{int}	0.0712	0.0823
Reflections measured	54965	8039
Reflections observed	21486	6667
Goodness-of-fit (GOF) on F^2	1.008	1.127
$R_1{}^a$	0.0623	0.0743
wR_2 (all data)^b	0.1785	0.2092
Largest differences peak and hole (e Å^{-3})	1.527 and −0.972	1.025 and −1.183

[a] $R_1 = \Sigma||F_0|-|F_c||/\Sigma|F_0|$.
[b] $wR_2 = \{\Sigma[w(||F_0|^2 - |F_c|^2|)^2]| / \Sigma[w(F_0^4)]\}^{1/2}$.

3. Results and discussion

3.1. Synthesis and characterization

Reaction of **L^3** or **L^4** [prepared *in situ* by the condensation of **L^1** or **L^2** and salicylaldehyde in the presence of triethylamine] and the corresponding hydrated Co(II), Ni(II), Cu(II) or Zn(II) salts (perchlorates or nitrates) in 2-propanol led to compounds of formula [M$_2$(L)](X)$_2$·$y$solv (M = Co, Ni, Cu or Zn). The IR and FAB-mass spectra confirmed the formation of the complexes with the corresponding Schiff-base lariat ether. The IR spectra (KBr disks) feature a band attributable to the v(C=N)$_{imine}$ stretching mode at 1606–1614 cm^{-1}. The presence of this band together with the absence of bands due to carbonyl and/or amine vibration modes confirms the formation of the imine. In the case of the perchlorate salts, bands corresponding to the v_{as}(Cl–O) stretching and δ_{as}(O–Cl–O) bending modes of the perchlorate groups appear at *ca.* 1100 and 630 cm^{-1} [28]. The absorptions at *ca.* 630 cm^{-1} clearly show up without splitting, as befit uncoordinated anions. The IR spectra of the nitrate salts show an intense band at *ca.* 1384 cm^{-1} characteristic of ionic NO$_3^-$. The FAB-mass spectrum of each complex displays a rather intense peak corresponding to the [M$_2$(L)(X)]$^+$ fragment

(M = Co, Ni, Cu or Zn, X = ClO_4^- or NO_3^-), which indicates the formation of the desired binuclear complexes.

Table 2. Crystal data and structure refinement for **9b**, **14b** and **11**.

	9b	14b	11
Empirical formula	$C_{44}H_{52}Cl_2Co_2N_6O_{14}$	$C_{40}H_{46}Cu_2N_6O_{12}$	$C_{40}H_{46}Cl_2N_4O_{14}Zn_2$
Molecular weight	1077.68	929.91	1008.45
Temperature (K)	100.0(2)	298(2)	150.0(2)
Wavelength (Å)	0.71073	0.71073	0.71073
Crystal system	monoclinic	monoclinic	triclinic
Space group	$P2_1/c$	$P2_1/n$	$P1^-$
a (Å)	10.0689(15)	12.437(5)	9.971(4)
b (Å)	10.1689(15)	9.476(5)	11.020(4)
c (Å)	22.134(3)	17.096(12)	11.252(4)
α (°)	90	90	104.597(7)
β (°)	95.408(3)	95.01(3)	109.533(6)
γ (°)	90	90	105.709(6)
V (Å^3)	2256.2(6)	1999.8(19)	1019.9(7)
$F(0\,0\,0)$	1116	964	520
Z	2	2	1
Calculated density (g cm^{-3})	1.586	1.544	1.642
Absorption coefficient (mm^{-1})	0.930	1.136	1.382
θ Range for data collection (°)	1.85–28.29	1.92–27.14	2.07–27.48
R_{int}	0.0733	0.0638	0.0531
Reflections measured	14726	11822	11523
Reflections observed	2993	2576	3103
Goodness-of-fit (GOF) on F^2	1.025	0.981	1.065
$R_1{}^a$	0.0450	0.0576	0.0501
wR_2 (all data)^b	0.1003	0.1218	0.1244
Largest differences peak and hole (e Å^{-3})	0.47 and −0.603	0.31 and −0.277	0.59 and −0.711

^{a} $R_1 = \Sigma||F_0|-|F_c||/\Sigma|F_0|$.
^{b} $wR_2 = \{\Sigma[w(||F_0|^2 - |F_c|^2|)^2]| / \Sigma[w(F_0^4)]\}^{1/2}$.

3.2. X-ray crystal structures of L^3 complexes

The solid state structures of compounds **6b** and **7b** were determined by single crystal X-ray diffraction analyses. The asymmetric unit in crystals of **6b** contains two complex cations [Ni$_2$(L^3)(H$_2$O)$_2$]$^{2+}$ with slightly different bond distances and angles of the metal coordination environment, five nitrate anions, a triethylammonium cation and four water molecules. Inner-sphere water molecules are involved in hydrogen bonding interaction with nitrate anions and non coordinated water molecules. Nitrate anions are further involved in hydrogen bonding interactions with non coordinated water molecules and triethylammonium cations, giving rise to a complicated 3D hydrogen bonding network. Bond distances and angles of the metal coordination environments are given in Table 3, while a view of the structure of the complex cations is shown in Fig. 1. The metal ions are six-coordinate, being directly bound to a pivotal nitrogen atom, a

nitrogen atom of an imine group, two oxygen atoms of the crown moiety and an oxygen atom of the phenolate group. Coordination number six is completed by an oxygen atom of an inner-sphere water molecule. The metal ions show distorted octahedral coordination environments, the *trans* angles ranging from 164.6(6)° to 177.6(1)°, and the *cis* angles between 80.2(1)° and 95.3(1)°.

Table 3. Selected bond lengths (Å) and angles (°) for **6b**[a].

Ni(1)–O(1)	1.940(3)	Ni(2)–O(5)	1.946(3)
Ni(1)–N(1)	2.028(4)	Ni(2)–N(4)	2.037(4)
Ni(1)–N(2)	2.057(4)	Ni(2)–O(7)	2.051(3)
Ni(1)–O(6)	2.069(3)	Ni(2)–N(3)	2.053(3)
Ni(1)–O(3)	2.077(3)	Ni(2)–O(4)	2.134(3)
Ni(1)–O(2)	2.422(3)	Ni(2)–O(2)	2.426(3)
N(1)–Ni(1)–O(3)	173.1(1)	N(4)–Ni(2)–O(4)	172.5(1)
O(1)–Ni(1)–N(2)	168.9(1)	O(5)–Ni(2)–N(3)	169.5(1)
O(6)–Ni(1)–O(2)	173.7(1)	O(7)–Ni(2)–O(2)	177.0(1)
O(1)–Ni(1)–O(6)	93.9(1)	O(5)–Ni(2)–O(7)	90.3(1)
O(1)–Ni(1)–O(3)	91.4(1)	O(5)–Ni(2)–O(4)	92.1(1)
O(1)–Ni(1)–N(1)	93.6(1)	O(5)–Ni(2)–N(4)	94.4(1)
O(1)–Ni(1)–O(2)	92.0(1)	O(5)–Ni(2)–O(2)	91.8(1)
N(2)–Ni(1)–O(6)	93.7(1)	N(3)–Ni(2)–O(7)	96.4(1)
N(2)–Ni(1)–O(3)	81.0(1)	N(3)–Ni(2)–O(4)	80.2(1)
N(2)–Ni(1)–N(1)	94.8(1)	N(3)–Ni(2)–N(4)	93.7(1)
N(2)–Ni(1)–O(2)	80.2(1)	N(3)–Ni(2)–O(2)	81.3(1)
O(2)–Ni(1)–O(3)	91.6(1)	O(2)–Ni(2)–O(4)	91.8(1)
O(6)–Ni(1)–O(3)	85.8(1)	O(7)–Ni(2)–O(4)	86.0(1)
O(6)–Ni(1)–N(1)	89.0(1)	O(7)–Ni(2)–N(4)	90.4(1)
N(1)–Ni(1)–O(2)	93.0(1)	N(4)–Ni(2)–O(2)	91.6(1)

[a] Only the bond distances and angles of one of the complex cations present in the asymmetric unit are given.

In the $[Ni_2(L^3)(H_2O)_2]^{2+}$ cations the macrocyclic ligand adopts an *anti* conformation with the two pendant arms disposed on opposite sides of the crown moiety. One of the Ni(II) ions is placed above the mean square plane defined by the donor atoms of the crown moiety, while the second Ni(II) ion is placed below that plane. An oxygen atom of the crown moiety [O(2) or O(9), see Fig. 1] is acting as a bridge between the two metal ions, which are separated by *ca.* 4.3 Å. Weakly basic ether donors rarely bridge metal centers [29,30], and even the bridging role for THF, one of the most utilized ether-type ligands, is very uncommon in the solid state [31]. A simple search into the Cambridge Structural Data Base (Version V5.31 (2010)) shows only 26 entries for transition-metal complexes containing bridging ether donor atoms. Among these hits, 13 include THF bridging ligands and another 13 contain other oxygen ether bridges. Among the latter group seven entries correspond to silver complexes, three to mercury complexes and two cadmium complexes. Our search did not provide any nickel complex containing ether bridging ligands, while only one cobalt complex with a THF bridge [32], another cobalt complex with a different ether bridge [30] and one copper complex with a methyl ether bridging group [30] were found. The distance between the Ni(II) ions and the bridging ether oxygen atom is 0.29–0.48 Å longer than the remaining bond distances of the metal coordination

environments. The C–O(2)–C angle [109.7(3)°] is very close to the ideal tetrahedral value, while the C–O(3)–C [115.0(3)°] and C–O(4)–C [113.9(3)°] angles, which involve non bridging ether donor atoms, are considerably more open. The distance between the two Ni(II) ions amounts to 4.3 Å. The Ni–µ(O)–Ni angle is about 125°, while the distance between the two pivotal nitrogen atoms amounts to 5.68 Å.
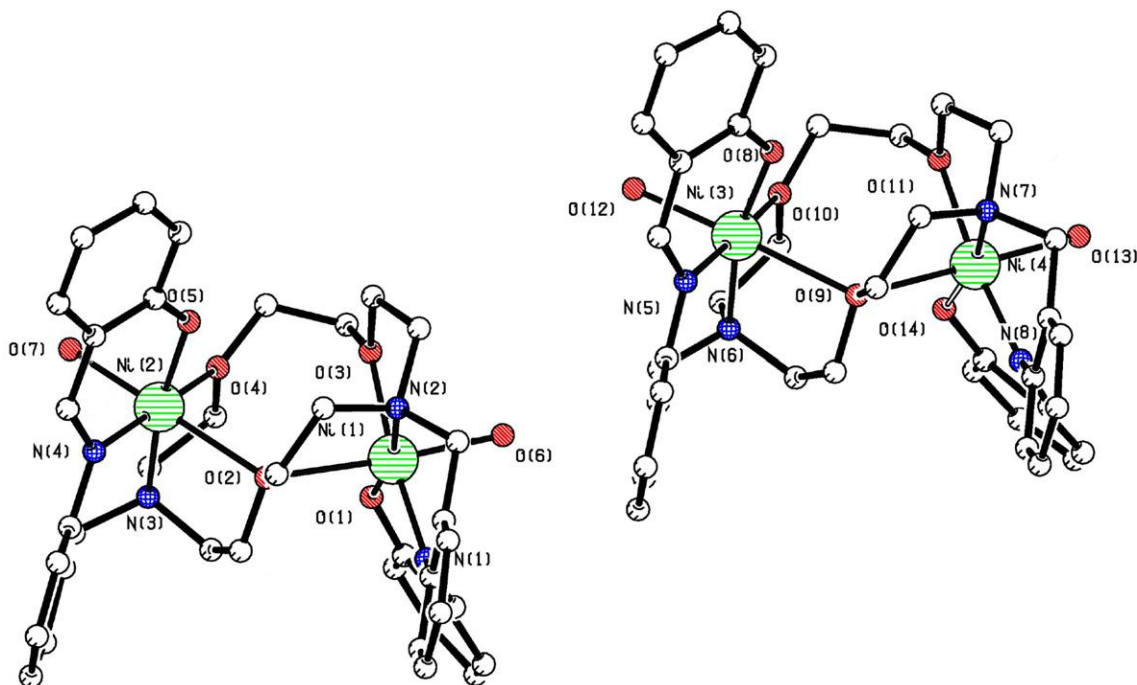

Fig. 1. PLUTON view of the two $[Ni_2(L^3)(H_2O)_2]^{2+}$ complex cations present in the asymmetric unit of **6b**.

Unlike the nickel compound, inspection of crystals of the copper analogue **7b** reveals the presence of a 1D cationic coordination polymer in which $[Cu_2(L^3)]^+$ units are liked by nitrate bridges. The crystal lattice also contains acetonitrile molecules and a well separated nitrate anion. Table 4 summarizes selected bond lengths and angles of the metal coordination environments, while the structure of the complex is depicted in Fig. 2. The Cu(II) ions are six-coordinate, being directly bound to a pivotal nitrogen atom, the nitrogen atom of the imine group, two oxygen atoms of the crown moiety, the oxygen atom of a phenolate group and an oxygen atom of a nitrate ligand. One of the ether oxygen atoms of the crown moiety is bridging the two Cu(II) ions, as observed for the Ni(II) analogue. The distance between the two Cu(II) ions in $[Cu_2(L^3)(NO_3)]^+$ units amounts to 4.305(1) Å, while the Cu–µ(O)–Cu angle is 114.3(1)°. The distance between Cu(II) ions of neighboring $[Cu_2(L^3)(NO_3)]^+$ complexes is 6.3358(9) Å. The metal coordination environments can be described as distorted octahedral, where the Jahn–Teller distortions occur through the O(7)–Cu(1)–O(4) and O(6)–Cu(2)–O(4) axes. Indeed, the Cu(1)–O(4), Cu(1)–O(7), Cu(2)–O(4) and Cu(2)–O(6) distances are *ca.* 0.50–0.71 Å longer than the remaining bond distances of the metal coordination environments. The *trans* angles vary between 164.6(1)° and 173.1(1)°, while the *cis* angles of the equatorial planes range between 77.0(1)° and 99.4(1)°.

Inspection of the crystal structure of **7b** also reveals the presence of intermolecular face to face π–π stacking interactions [33] between the benzyl units of neighboring $[Cu_2(L^3)(NO_3)]^+$ units (Fig. 2). The distance between the centers of these rings is 3.6 Å, while the dihedral angle between the least squares planes amounts to 8.28°.

Table 4. Selected bond lengths (Å) and angles (°) for **7b**.

Cu(1)–O(1)	1.884(3)	Cu(2)–O(5)	1.878(3)
Cu(1)–N(1)	1.975(4)	Cu(2)–N(4)	1.982(4)
Cu(1)–O(2)	2.029(3)	Cu(2)–O(3)	2.044(3)
Cu(1)–N(2)	2.030(3)	Cu(2)–N(3)	2.020(4)
Cu(1)–O(7)	2.586(4)	Cu(2)–O(6)	2.566(3)
Cu(1)–O(4)	2.531(3)	Cu(2)–O(4)	2.592(3)
N(1)–Cu(1)–O(2)	173.1(1)	N(4)–Cu(2)–O(3)	170.7(1)
O(1)–Cu(1)–N(2)	170.1(1)	O(5)–Cu(2)–N(3)	168.6(1)
O(7)–Cu(1)–O(4)	164.6(1)	O(6)–Cu(2)–O(4)	169.5(1)
N(1)–Cu(1)–N(2)	96.5(1)	N(4)–Cu(2)–N(3)	96.9(1)
N(1)–Cu(1)–O(4)	93.3(1)	N(4)–Cu(2)–O(6)	90.7(1)
O(1)–Cu(1)–N(1)	93.2(1)	O(5)–Cu(2)–N(4)	93.9(1)
O(7)–Cu(1)–N(1)	81.3(1)	O(4)–Cu(2)–N(4)	93.5(1)
O(7)–Cu(1)–N(2)	88.4(1)	O(4)–Cu(2)–N(3)	77.0(1)
O(7)–Cu(1)–O(2)	91.9(1)	O(4)–Cu(2)–O(3)	95.1(1)
O(7)–Cu(1)–O(1)	95.4(1)	O(4)–Cu(2)–O(5)	98.7(1)
O(2)–Cu(1)–N(2)	81.9(1)	O(3)–Cu(2)–N(3)	81.8(1)
O(4)–Cu(1)–N(2)	77.8(1)	O(6)–Cu(2)–N(3)	93.0(1)
O(1)–Cu(1)–O(2)	88.8(1)	O(5)–Cu(2)–O(3)	88.2(1)
O(4)–Cu(1)–O(2)	92.9(1)	O(6)–Cu(2)–O(3)	80.2(1)
O(4)–Cu(1)–O(1)	99.4(1)	O(6)–Cu(2)–O(5)	90.5(1)

3.3. X-ray crystal structures of L^4 complexes

The solid state structures of compounds **9b**, **14b** and **11** were also determined by single crystal X-ray diffraction analyses. Crystals of **9b** contain the cation $[Co_2(L^4)(CH_3CN)_2]^{2+}$ and two well-separated perchlorate anions, while those of **14b** and **11** contain cations $[M_2(L^4)]^{2+}$ (M = Cu or Zn) and two uncoordinated (nitrate or perchlorate) anions. Table 5 summarizes selected bond lengths and angles of the metal coordination environments, while the structures of the cations are depicted in Fig. 3, Fig. 4, Fig. 5. In all cases, the macrocyclic ligand adopts an *anti* conformation in the complexes, with the two pendant arms disposed on opposite sides of the crown moiety. The asymmetric unit comprises a half complex cation and one anion and, as a consequence, the two metal ions within a complex cation are centrosymmetrically related and possess identical coordination environments. Unlike in the L^3 analogues, none of the oxygen atoms of the crown moiety is acting as a bridging donor atom in the $[Co_2(L^4)(CH_3CN)_2]^{2+}$, $[Cu_2(L^4)]^{2+}$ and $[Zn_2(L^4)]^{2+}$ complexes. This is attributed to the larger size of the crown moiety and the presence of an additional oxygen donor atom in L^4 compared to L^3.

In the Co(II) complex the metal ions are six-coordinate, being directly bound to a pivotal nitrogen atom [N(2)], the nitrogen atom of the imine group, N(1), two oxygen atoms of the crown moiety, [O(2) and O(3)], and the oxygen atom of the phenolate group [O(1)]. Coordination number six is completed by a nitrogen atom of an acetonitrile molecule. The metal ions present a distorted octahedral coordination environment; the *trans* angles O(1)–Co(1)–N(2) [173.7(1)°], N(1)–Co(1)–O(3) [168.8(1)°] and O(2)–Co(1)–N(3) [172.3(1)°] are close to 180°, while the *cis* angles in the corresponding equatorial planes range between 79.4(1)° and 97.3(1)°. The mean deviation from planarity of the three equatorial planes are 0.095(3) Å [Co(1)N(1)N(3)O(2)O(3)], 0.061(3) Å [Co(1)N(2)N(3)O(1)O(2)] and 0.092(3) Å [Co(1)N(1)N(2)O(1)O(3)].
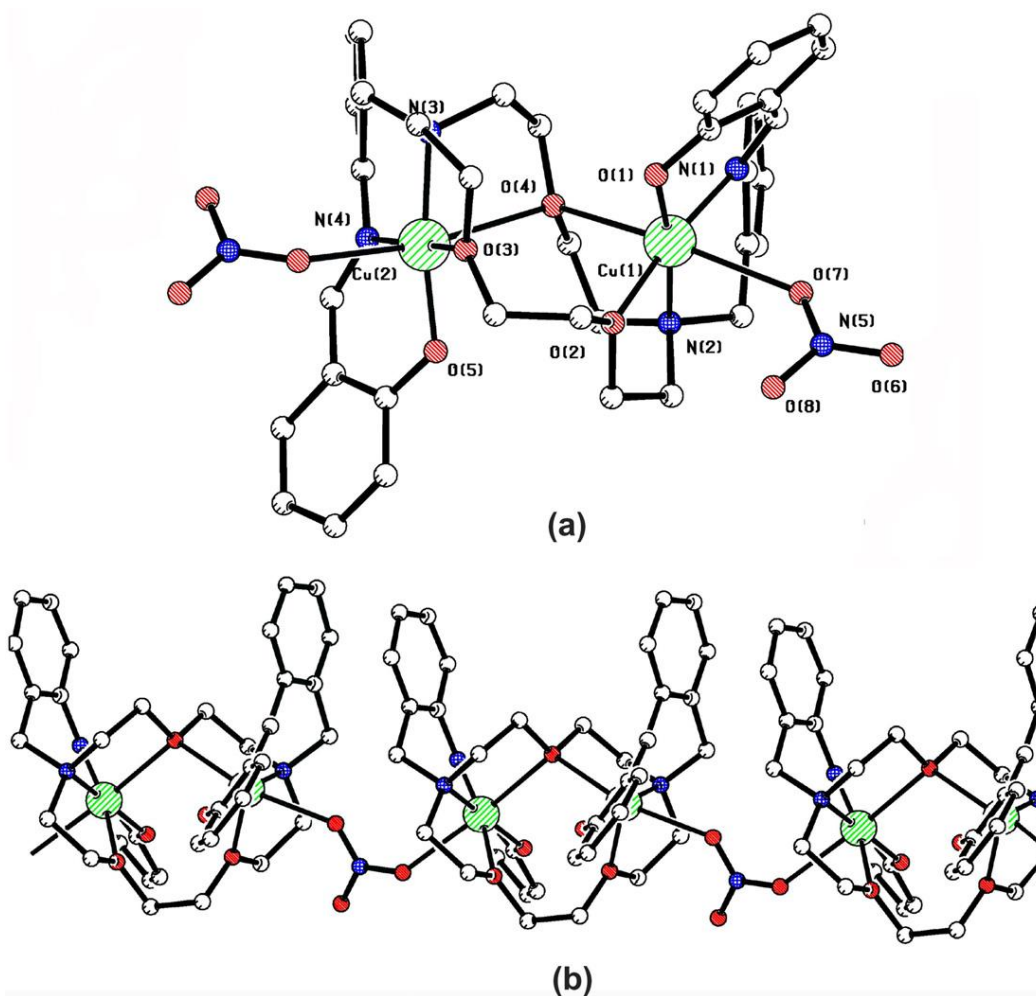
Fig. 2. (a) PLUTON view of the $\{[Cu_2(L^3)(NO_3)]^+\}$ unit present in crystals of **7b**. (b) View of the $\{[Cu_2(L^3)(NO_3)]^+\}_n$ coordination polymer present in crystals of **7b**.
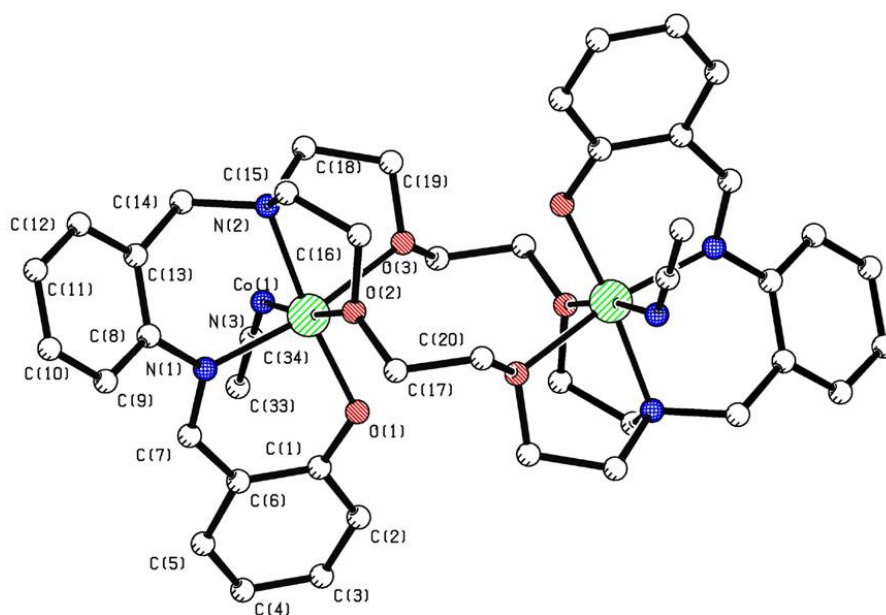

Fig. 3. PLUTON view of the $[Co_2(L^4)(CH_3CN)_2]^{2+}$ complex cation present in crystals of **9b**.

Table 5. Selected bond lengths (Å) and angles (°) for **9b**, **14b** and **11**.

9b		14b		11	
Co(1)–O(1)	1.944(2)	Cu(1)–O(1)	1.864(3)	Zn(1)–O(1)	1.905(3)
Co(1)–N(1)	2.070(3)	Cu(1)–N(1)	1.961(3)	Zn(1)–N(1)	2.060(3)
Co(1)–O(2)	2.116(2)	Cu(1)–N(2)	1.999(3)	Zn(1)–N(2)	3.076(3)
Co(1)–N(2)	2.127(3)	Cu(1)–O(2)	2.154(3)	Zn(1)–O(2)	2.170(3)
Co(1)–O(3)	2.170(2)	Cu(1)–O(3)	2.169(3)	Zn(1)–O(3)	2.240(2)
Co(1)–N(3)	2.266(3)				
O(1)–Co(1)–N(1)	92.5(1)	N(2)–Cu(1)–O(2)	82.0(1)	N(2)–Zn(1)–O(2)	77.9(1)
O(1)–Co(1)–O(2)	96.1(1)	O(1)–Cu(1)–O(3)	96.4(1)	O(1)–Zn(1)–O(3)	93.2(1)
N(1)–Co(1)–O(2)	97.3(1)	N(1)–Cu(1)–O(3)	123.9(1)	N(1)–Zn(1)–O(3)	123.6(1)
O(1)–Co(1)–N(2)	173.7(1)	N(2)–Cu(1)–O(3)	79.5(1)	N(2)–Zn(1)–O(3)	78.4(1)
N(1)–Co(1)–N(2)	92.5(1)	O(2)–Cu(1)–O(3)	105.0(1)	O(2)–Zn(1)–O(3)	113.82(9)
O(2)–Co(1)–N(2)	79.4(1)	N(1)–Cu(1)–N(2)	95.2(1)	N(1)–Zn(1)–N(2)	94.7(1)
O(1)–Co(1)–O(3)	95.39(9)	O(1)–Cu(1)–O(2)	90.7(1)	O(1)–Zn(1)–O(2)	99.6(1)
N(1)–Co(1)–O(3)	168.8(1)	O(1)–Cu(1)–N(1)	94.4(1)	O(1)–Zn(1)–N(1)	95.8(1)
O(2)–Co(1)–O(3)	89.73(9)	O(1)–Cu(1)–N(2)	170.2(1)	O(1)–Zn(1)–N(2)	169.1(1)
N(2)–Co(1)–O(3)	80.2(1)	N(1)–Cu(1)–O(2)	129.7(1)	N(1)–Zn(1)–O(2)	119.2(1)
O(1)–Co(1)–N(3)	89.9(1)				
N(1)–Co(1)–N(3)	87.2(1)				
O(2)–Co(1)–N(3)	172.3(1)				
N(2)–Co(1)–N(3)	94.3(1)				
O(3)–Co(1)–N(3)	85.0(1)				
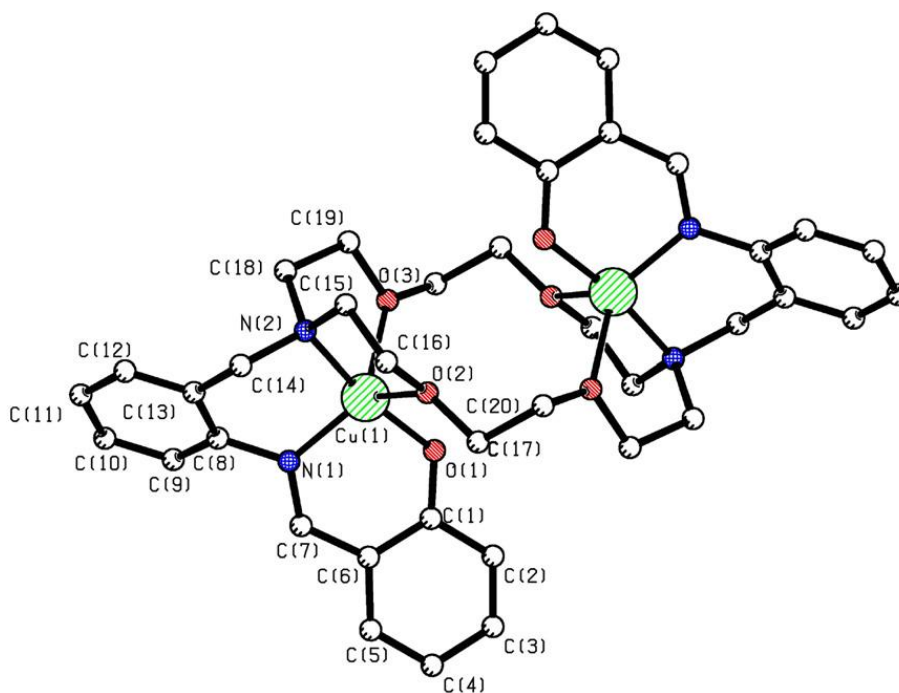
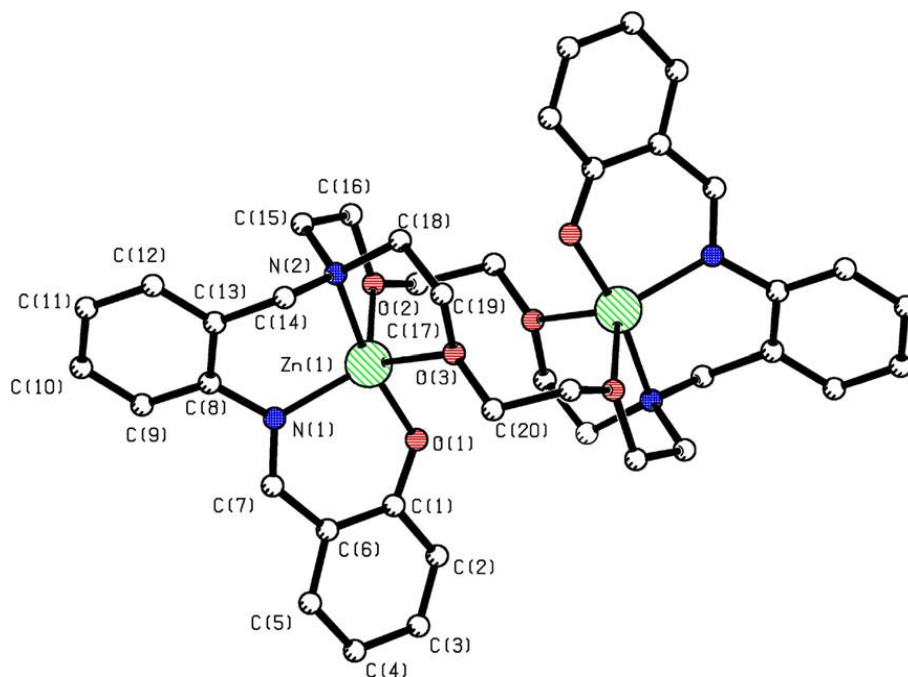**Fig. 4.** PLUTON view of the [Cu₂(L⁴)]²⁺ complex cation present in crystals of **14b**.

Fig. 5. PLUTON view of the $[Zn_2(L^4)]^{2+}$ complex cation present in crystals of **11**.

In the Cu(II) and Zn(II) complexes the metal ions are five-coordinate, being directly bound to a pivotal nitrogen atom [N(2)], the nitrogen atom of the imine group, N(1), two oxygen atoms of the crown moiety, [O(2) and O(3)], and the oxygen atom of the phenolate group [O(1)]. The metal ions show a distorted trigonal–bipyramidal coordination environment, as indicated from the value of the index of trigonality τ of 0.68 (**14b**) and 0.76 (**11**) ($\tau = 0$ for a perfect square-pyramidal geometry and $\tau = 1$ for a regular trigonal bipyramidal geometry) [34,35]. The equatorial plane of the trigonal-bipyramid can be considered to be comprised by the two oxygen atoms of the crown moiety and the nitrogen atom of the imine group, while the pivotal nitrogen atom and the oxygen atom of the phenolate group occupy the apical positions. The angles of the equatorial plane [N(1)–M(1)–O(2), N(1)–M(1)–O(3) and O(2)–M(1)–O(3), Table 3] are relatively close to the ideal value expected for a regular trigonal-bipyramidal coordination (120°), while the N(2)–M(1)–O(1) angles deviate by *ca.* 10° from the expected value (180°).

It is important to note that the coordination environment around the metal ion found in **14b** is somewhat different than that observed in the analogous perchlorate salt [16]. The bond distances of the metal coordination environment are very similar for both compounds with the exception of the Cu–O(3) distance, which amounts to 2.169(3) Å in **14b** and to 2.359(3) Å in the perchlorate analogue. These two compounds also show significant differences in some of the bond angles of the metal coordination environment. The main differences affect to the N(1)–Cu(1)–O(2) and N(1)–Cu(1)–O(3) angles, which amount to 129.7(1)° and 123.9(1)° in **14b** and 145.9(2)° and 107.3(1)° in the perchlorate salt, respectively. These values indicate a larger deviation from the expected values for a perfect trigonal-bipyramidal coordination (120°) in the case of the perchlorate analogue, which results in a value of the index of trigonality indicating an intermediate coordination between a square-pyramidal and a trigonal-bipyramidal coordination ($\tau = 0.40$).

4. **Conclusions**

A series of binuclear Ni(II), Co(II), Cu(II) and Zn(II) complexes based on 1,10-diaza-15-crown-5 or 4,13-diaza-18-crown-6 platforms have been synthesized and characterized. The solid state structures of the Ni(II)

and Cu(II) complexes of the smaller ligand L^3 show a quite rare feature, as an ether oxygen atom of the crown moiety is bridging the two metal ions. This situation is not observed for the complexes of L^4 as a consequence of the higher denticity of this ligand and the larger size of its crown moiety.

Acknowledgements

Supplementary data

CCDC 770663, 770665, 770664, 770661 and 77662 contain the supplementary crystallographic data for (**6b**), (**7b**), (**9b**), (**11**) and (**14b**). These data can be obtained free of charge via http://www.ccdc.cam.ac.uk/conts/retrieving.html, or from the Cambridge Crystallographic Data Centre, 12 Union Road, Cambridge CB2 1EZ, UK; fax: (+44) 1223-336-033; or e-mail: deposit@ccdc.cam.ac.uk.

References

[1] H. Miyasaka, A. Sayito, S. Abe, Coord. Chem. Rev. 251 (2007) 2622.

[2] K.C. Gupta, A.K. Sutar, Coord. Chem. Rev. 252 (2008) 1420.

[3] D.E. Fenton, Chem. Soc. Rev. 28 (1999) 159.

[4] G. Consiglio, S. Failla, I.P. Oliveri, R. Purrello, S. Di Bella, Dalton Trans. (2009) 10426.

[5] B. Dede, I. Ozmen, F. Karipcin, Polyhedron 28 (2009) 3967.

[6] A.L. Gavrilova, B. Bosnich, Inorg. Chim. Acta 352 (2003) 24.

[7] C. Liu, M. Wang, T. Zhang, H. Sun, Coord. Chem. Rev. 248 (2004) 147.

[8] S. Alvarez, A.A. Palacios, G. Aullon, Coord. Chem. Rev. 185–186 (1999) 431.

[9] L. Vaiana, C. Platas-Iglesias, D. Esteban-Gomez, F. Avecilla, A. de Blas, T. Rodríguez-Blas, Eur. J. Inorg. Chem. (2007) 1874.

[10] C. Platas-Iglesias, D. Esteban, V. Ojea, F. Avecilla, A. de Blas, T. Rodríguez-Blas, Inorg. Chem. 42 (2003) 4299.

[11] D. Esteban, D. Bañobre, A. de Blas, T. Rodríguez-Blas, R. Bastida, A. Macías, A. Rodríguez, D.E. Fenton, H. Adams, J. Mahía, Eur. J. Inorg. Chem. (2000) 1445.

[12] D. Esteban, F. Avecilla, C. Platas-Iglesias, J. Mahía, A. de Blas, T. Rodríguez-Blas, Inorg. Chem. 41 (2002) 4337.

[13] D. Esteban, F. Avecilla, C. Platas-Iglesias, A. de Blas, T. Rodríguez-Blas, Polyhedron 22 (2003) 2709.

[14] L. Vaiana, C. Platas-Iglesias, D. Esteban-Gómez, F. Avecilla, J.M. Clemente-Juan, J.A. Real, A. de Blas, T. Rodríguez-Blas, Dalton Trans. (2005) 2031.

[15] C. Platas-Iglesias, L. Vaiana, D. Esteban-Gómez, F. Avecilla, J.A. Real, A. de Blas, T. Rodríguez-Blas, Inorg. Chem. 44 (2005) 9704.

[16] C. Rodríguez-Infante, D. Esteban, F. Avecilla, A. de Blas, T. Rodríguez-Blas, J. Mahia, A.L. Macedo, C.F.G.C. Geraldes, Inorg. Chim. Acta 317 (2001) 190.

[17] C. Platas, F. Avecilla, A. de Blas, T. Rodríguez-Blas, R. Bastida, A. Macias, A. Rodríguez, H. Adams, J. Chem. Soc., Dalton Trans. (2001) 1699.

[18] M. Gonzalez-Lorenzo, C. Platas-Iglesias, F. Avecilla, C.F.G.C. Geraldes, D. Imbert, J.-C.G. Bünzli, A. de Blas, T. Rodríguez-Blas, Inorg. Chem. 42 (2003) 6946.

[19] D. Esteban-Gomez, C. Platas-Iglesias, T. Enriquez-Perez, F. Avecilla, A. de Blas, T. Rodríguez-Blas, Inorg. Chem. 45 (2006) 5407.

[20] D. Esteban-Gomez, C. Platas-Iglesias, F. Avecilla, A. de Blas, T. Rodríguez-Blas, Eur. J. Inorg. Chem. (2007) 1635.

[21] D. Esteban-Gomez, R. Ferreiros, S. Fernandez-Martinez, F. Avecilla, C. Platas-Iglesias, A. de Blas, T. Rodríguez-Blas, Inorg. Chem. 44 (2005) 5428.

[22] D. Esteban-Gomez, C. Platas-Iglesias, A. de Blas, L. Fabbrizzi, T. Rodríguez-Blas, Chem. Eur. J. 14 (2008) 5829.

[23] D. Esteban, D. Bañobre, A. de Blas, T. Rodríguez-Blas, R. Bastida, A. Macias, A. Rodríguez, D.E. Fenton, H. Adams, J. Mahia, Eur. J. Inorg. Chem. (2000) 1445.

[24] L.J. Farrugia, J. Appl. Cryst. 32 (1999) 837.

[25] P.T. Beurskens, G. Beurskens, R. de Gelder, S. Garcia-Granda, R.O. Gould, R. Israel, J.M.M. Smits, DIRDIF99 Program System, Crystallography Laboratory, University of Nijmegen, The Netherlands, 1999.

[26] M.C. Burla, M. Camalli, B. Carrozzini, G.L. Cascarano, C. Giacovazzo, G. Polidori, R. Spagna, SIR2002: J. Appl. Cryst. 36 (2003) 1103.

[27] G.M. Sheldrick, SHELX97 – Programs for Crystal Structure Analysis (Release 97-2). Institüt für Anorganische Chemie der Universität, Tammanstrasse 4, D-3400 Göttingen, Germany, 1998.

[28] K. Nakamoto, Infrared and Raman Spectra of Inorganic and Coordination Compounds, third ed., J. Wiley, New York, Chichester, Brisbane and Toronto, 1972. pp. 142–154.

[29] A. Roth, J. Becher, C. Herrmann, H. Gorls, G. Vaughan, M. Reiher, D. Klemm, W. Plass, Inorg. Chem. 45 (2006) 10066.

[30] G. Mund, A.J. Gabert, R.J. Batchelor, J.F. Britten, D.B. Leznoff, Chem. Commun. (2002) 2990.

[31] M. Doring, G. Hahn, M. Stoll, A.C. Wolski, Organometallics 16 (1997) 1879.

[32] R. Crescenzi, E. Solari, C. Floriani, A. Chiesi-Villa, C. Rizzoli, Inorg. Chem. 35 (1996) 2413.

[33] C.A. Hunter, J.K.M. Sanders, J. Am. Chem. Soc. 112 (1990) 5225.

[34] The parameter s is the index of the degree of trigonality within the structural continuum between square-pyramidal and trigonal-bipyramidal geometries. If A is the apical donor atom of a square-based pyramid then it should not be amongst the atoms which define the largest two angles at the metal center. Donor atoms B

and C are associated with the greater basal angle (b) and atoms D and E with the smaller basal angle (a); $s = (b - a)/60$ and is therefore 0 for a square pyramid and 1 for a trigonal-bipyramid.

[35] A.W. Addison, T. Nageswara-Rao, J. Reedijk, J. van Rijn, G.C. Verschoor, J. Chem. Soc., Dalton Trans. (1984) 1349.